Lactosylceramide: Effect of Acyl Chain Structure on Phase Behavior and Molecular Packing

Xin-Min Li, Maureen M. Momsen, Howard L. Brockman, and Rhoderick E. Brown
The Hormel Institute, University of Minnesota, Austin, Minnesota 55912 USA

ABSTRACT Lactosylceramide (LacCer) is a pivotal intermediate in the metabolism of higher gangliosides, localizes to sphingolipid-sterol "rafts," and has been implicated in cellular signaling. To provide a fundamental characterization of LacCer phase behavior and intermolecular packing, LacCer containing different saturated (16:0, 18:0, 24:0) or monounsaturated ($18{:}1^{\Delta 9}$, $24{:}1^{\Delta 15}$) acyl chains were synthesized and studied by differential scanning calorimetry and Langmuir film balance approaches. Compared to related sphingoid- and glycerol-based lipids, LacCers containing saturated acyl chains display relatively high thermotropic and pressure-induced transitions. LacCer monolayer films are less elastic in an in-plane sense than sphingomyelin films, but are somewhat more elastic than galactosylceramide films. Together, these findings indicate that the disaccharide headgroup only marginally disrupts gel phase packing and orients more perpendicular than parallel to the interface. This contrasts the reported behavior of digalactosyldiglycerides with saturated acyl chains. Introducing single *cis* double bonds into the LacCer acyl chains dramatically lowers the high thermotropic and pressure-induced transitions. Greater reductions occur when *cis* double bonds are located near the middle of the acyl chains. The results are discussed in terms of how an extended disaccharide headgroup can enhance interactions among naturally abundant LacCers with saturated acyl chains.

INTRODUCTION

Glycosphingolipids (GSLs) have been implicated in cell-cell interaction and recognition processes such as adhesion, differentiation, development, and transformation (e.g., Pincet et al., 2001; Hakomori and Igarashi, 1995; Weis and Drickamer, 1996) and serve as membrane receptors for toxins, drugs, and natural agonists. Among GSLs, lactosylceramide (LacCer) is a pivotal intermediate in the degradation and synthesis of many complex GSLs including gangliosides (i.e., GM3, ABO blood-type, and globo-type) (Chen et al., 1999; Huwiler et al., 2000; van Meer and Holthuis, 2000). LacCer has been implicated in cell-cell and cell-matrix interactions and in signaling events linked to cell differentiation, development, apoptosis, and oncogenesis. LacCer stimulates the expression of CD11/CD8, or Mac-1, on the surface of human neutrophils and orchestrates a signal transduction pathway that leads to vascular endothelial cell proliferation by a redox-dependent transcriptional pathway that is mediated by the expression of tumor necrosis factor α (TNF-α)-induced nuclear factor κB (NF-κB) and intercellular adhesion molecule (ICAM-1) (Chatterjee, 1998). LacCer appears to be essential for osteoclastogenesis mediated by macrophage-colony stimulating factor and to be a receptor activator of NF-κB ligand (Iwamoto et al., 2001). This glycolipid also functions as an attachment site of *Helicobacter pylori,* a causative agent of gastric ulceritis (Angstrom et al., 1998).

Among GSLs, LacCer is highly enriched in sphingolipid-sterol microdomains isolated from biomembranes by Triton X-100 extraction of cells (Brown and Rose, 1992). These liquid-ordered microdomains, i.e., rafts, are believed to function as organizing platforms for various lipid-anchored proteins and to play a key role in transmembrane signaling processes (Simons and Ikonen, 1997; Brown, 1998; Brown and London, 1998, 2000; Simons and Toomre, 2000). LacCer recently has been identified as a crucial sphingolipid component of rafts in kidney cortex microvillar membranes based on its ability to enhance the detergent insolubility of glycosylphosphatidylinositol (GPI)-anchored dipeptidase (Parkin et al., 2001).

Because of the important functional roles attributed to LacCer in cells, gaining insight into the structural basis of this sphingolipid's physicochemical behavior is of timely importance. Current information about LacCer's physical behavior is quite limited. Most earlier studies of LacCer are complicated by acyl heterogeneity issues that are typical of many lipids isolated from biological tissues (e.g., Maggio, 1994; Maggio et al., 1978, 1980, 1981; Yu et al., 1997). A recent study, focusing on LacCer containing palmitoyl acyl chains, provided the first comprehensive characterization of LacCer phase structure by x-ray diffraction and differential scanning calorimetry (Saxena et al., 2000). What remains unclear is just how strongly changes in acyl length and saturation affect the phase behavior of LacCer, which has a disaccharide polar headgroup.

Here, we synthesized LacCer containing different homogeneous acyl chains commonly found in natural LacCer and investigated the effect of changing ceramide chain structure on the thermotropic and interfacial behavior by differential

Submitted March 6, 2002, and accepted for publication May 7, 2002.

Address reprint requests to Dr. Rhoderick E. Brown, The Hormel Institute, University of Minnesota, 801 16th Avenue NE, Austin, MN 55912. Tel.: 507-433-8804; Fax: 507-437-9606; E-mail: reb@tc.umn.edu.

Portions of this investigation were presented at the 46th Annual Meeting of the Biophysical Society held in San Francisco, CA. (Feb. 23–27, 2002)

0006-3495/02/09/1535/12 $2.00

scanning calorimetry (DSC) and by the Langmuir film balance approach, respectively. These approaches yield fundamental insights into the thermodynamic parameters of the lipid packing and phase behavior under conditions where the lipids are organized in planar arrays at the aqueous interface, a situation that mimics their arrangements in biological membranes. For phospholipids, it is well recognized that the phase behavior of lipid bilayers correlates well with two-dimensional molecular packing as a function of monolayer surface pressure (Phillips and Chapman, 1968; Albon and Baret, 1983; Peters and Beck, 1983). This also is the case for GSLs that exhibit different monolayer states depending on surface pressure, temperature, and the oligosaccharide chain type (Fidelio et al., 1986). We discuss the results obtained for LacCer within the context of established physicochemical parameters of related sphingoid-based and glycerol-based glycolipids.

MATERIALS AND METHODS

LacCer synthesis

LacCer with homogeneous acyl chains was produced by reacylating D-lactosyl-β1–1′-D-*erythro*-*s*phingosine (lyso LacCer; Avanti Polar Lipids, Alabaster, AL) with the desired fatty acyl residue as described previously (Smaby et al., 1996a and references therein). Briefly, the *N*-hydroxy succinimide ester of the desired fatty acid was prepared, recrystallized, and reacted with lyso-LacCer. Reacylation was performed at 60°C under nitrogen for 6–8 h in the presence of the catalyst, *N*-ethyldiisopropylamine. Following reacylation, LacCer was purified by flash column chromatography and crystallized from $CHCl_3/CH_3OH$ using −20°C acetone. Using the preceding approach, we prepared *N*-hexadecanoyl lactosylsphingosine (16:0 LacCer), *N*-octadecanoyl lactosylsphingosine (18:0 LacCer), *N*-tetracosanoate lactosylsphingosine (24:0 LacCer), *N*-cis-9-octadecenoate lactosylsphingosine (18:1 LacCer), and *N*-cis-15-tetracosenoate lactosylsphingosine (24:1 LacCer). *N*-octanoyl lactosylsphingosine (8:0 LacCer) was obtained from Avanti Polar Lipids. LacCer purity and *N*-acyl homogeneity were confirmed by TLC and by capillary gas chromatography, respectively. Final stock concentrations were determined by dry weight using a Cahn microbalance (model 4700).

Preparation of lipid dispersions for DSC

Lipid dispersions were prepared in phosphate buffer (pH 6.6) containing 10 mM potassium phosphate, 100 mM sodium chloride, and 1.5 mM sodium azide as described by Kulkarni et al. (1995, 1998). Briefly, phosphate buffer was added to the vacuum-dried lipid, which was then incubated above 90°C for 5 min and vortexed vigorously. This process was repeated two more times. Then, the dispersion was subjected to four freeze-thaw cycles to obtain a uniform distribution of buffer solutes across the bilayers (Mayer et al., 1985). Rapid freezing was achieved by immersing the lipid suspension in an isopropanol bath cooled by dry ice. During each thawing cycle, the LacCer dispersion was raised above 90°C and vortexed before subsequent freezing. Before loading into the calorimeter cell, the LacCer dispersion was degassed and then incubated at 5°C for 3 h before initiating the first heating scan.

Differential scanning calorimetry (DSC)

All thermotropic scans were obtained using a high-sensitivity MC-2 differential scanning calorimeter (Microcal, Amherst, MA) equipped with a DT-2801 data acquisition board for automated and computer-controlled data collection. The microcalorimeter was calibrated using three different high-purity phospholipids (dimyristoyl phosphatidylcholine, dipalmitoyl phosphatidylcholine, and dibehenoyl phosphatidylcholine) which have established phase transitions encompassing the range of 23–73°C. All thermograms depict heating mode scans performed at a rate of 10°C/h. The heat capacity (cal/°C) versus temperature output of the reference buffer was subtracted from that of the sample and then normalized for the lipid concentration using the ORIGIN data analysis package (Microcal). Transition temperatures (T_m) and enthalpies (ΔH) were determined from the peak midpoints and by integrating the peak areas, respectively, after applying the ORIGIN 2.9 non-two-state model with zero DCp. Note that highly cooperative endothermic transitions are followed by very sharp downward spikes projecting below the baseline (e.g., see Fig. 2: 16:0 LacCer). These spikes disappear upon sample dilution and do not appear to be of true exothermic origin.

Monolayer conditions

Stock solutions were prepared by dissolving LacCer in toluene/ethanol (5:6) or hexane/isopropanol/water (70:30:2.5). Solvent purity was checked by dipole potential measurements using a ^{210}Po ionizing electrode (Smaby and Brockman, 1991). Water for the subphase buffer was purified by reverse osmosis, activated charcoal adsorption, mixed-bed deionization, then passed through a Milli-Q UV Plus System (Millipore Corp., Bedford, MA), and filtered through a 0.22 μm Millipak 40 membrane. Subphase buffer (pH 6.6) consisting of 10 mM potassium phosphate, 100 mM NaCl, and 0.2% NaN_3 was stored under argon until use. Glassware was acid-cleaned, rinsed thoroughly with deionized water, and then with hexane/ethanol (95:5) before use.

Surface pressure-molecular area (π-A) isotherms were measured using a computer-controlled, Langmuir-type film balance, calibrated according to the equilibrium spreading pressures of known lipid standards (Momsen et al., 1990). Lipids were mixed and then spread (51.67 μl aliquots) from their dissolved stock solutions (see above). Films were compressed at a rate of ≤4 Å^2/molecule/min after an initial delay period of 4 min. The subphase was maintained at fixed temperature via a thermostated, circulating water bath. The film balance was housed in an isolated laboratory supplied with clean air by a Bioclean Air Filtration system equipped with charcoal and HEPA filters. The trough was separately enclosed under humidified argon, cleaned by passage through a seven-stage series filtration set-up consisting of an Alltech activated charcoal gas purifier, a LabClean filter, and a series of Balston disposable filters consisting of two adsorption (carbon) and three filter units (93% and 99.99% efficiency at 0.1 μm). Other features contributing to isotherm reproducibility include automated lipid spreading via a modified HPLC autoinjector, automated surface cleaning by multiple barrier sweeps between runs, and highly accurate and reproducible setting of the subphase level by an automated aspirator.

Analysis of isotherms

In keeping with recent proposals, we avoid using the term "liquid condensed" and instead use the term "condensed" to denote monolayers states in which the hydrocarbon chains are ordered (Kaganer et al., 1999). The "liquid-expanded" state differs from the condensed state in that the chains are conformationally disordered. Monolayer data were analyzed using Film Fit (Creative Tension, Inc., Austin, MN). Monolayer phase transitions between the liquid-expanded and condensed states were identified from the second and third derivatives of surface pressure (π) with respect to molecular area (A) (Ali et al., 1998; Li et al., 2000). Monolayer compress-

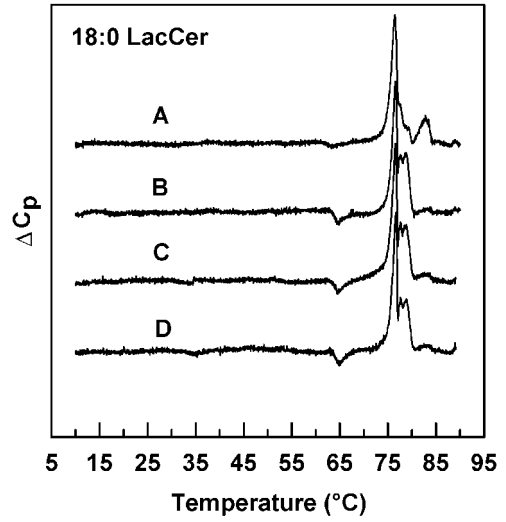

FIGURE 1 DSC of 18:0 LacCer. All traces represent heating scans obtained at a rate of 10°C/h. (*A*) Freshly prepared 18:0 LacCer dispersions incubated 3 h at 5°C before initiating the heating scan; (*B*) 18:0 LacCer dispersions incubated for 100 min at 5°C following an initial heating scan as described in *A*; (*C*) 18:0 LacCer dispersions incubated for 12 h at 5°C following the second heating scan as described in *B*; (*D*) 18:0 LacCer dispersions incubated for 4 days at room temperature (23°C) following the heating scan described in *C*.

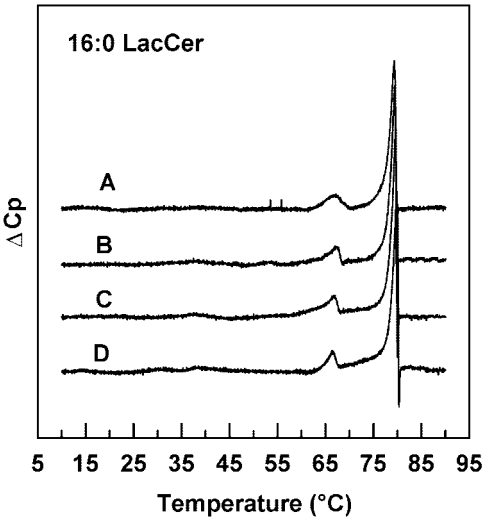

FIGURE 2 DSC of 16:0 LacCer. All traces represent heating scans obtained at a rate of 10°C/h. (Incubation times and temperatures are the same as described in Fig. 1 legend.)

ibilities at the indicated experimental mixing ratios were obtained from π-A data using:

$$C_s = (-1/A)(dA/d\pi) \quad (1)$$

where A is the area per molecule at the indicated surface pressure, π (e.g., Davies and Rideal, 1963; Behroozi, 1996). To facilitate comparing with elastic moduli of area compressibility values in bilayer systems (e.g., Evans and Needham, 1987; Needham and Nunn, 1990), we expressed our data as the reciprocal of C_s, originally defined as the surface compressional modulus (C_s^{-1}) by Davies and Rideal (1963). We used a 100-point sliding window that utilized every fourth point to calculate a C_s^{-1} value before advancing the window one point. Reducing the window size by as much as fivefold did not significantly affect the C_s^{-1} values obtained. Each C_s^{-1} versus average molecular area curve consisted of 200 C_s^{-1} values obtained at equally spaced molecular areas along the π-A isotherms. The standard error of the C_s^{-1} values is ~2%. High C_s^{-1} values correspond to low in-plane elasticity among packed lipids forming the monolayer. Recently, we characterized the response of C_s^{-1} to changes in lipid structure and phase state, as well as mixing interactions with cholesterol (Smaby et al., 1996b, 1997; Ali et al., 1998; Li et al., 2000, 2001, 2002). For comprehensive reviews of model membrane mechanoelastic properties, readers are referred to Needham (1995) and Behroozi (1996).

RESULTS

18:0 LacCer and 16:0 LacCer

Fig. 1 shows DSC heating scans of aqueous dispersions of 18:0 LacCer obtained after incubating in various ways before scanning. We found reproducibility to be improved by preparing LacCer multilamellar dispersions using a freeze-thaw and heating protocol previously reported to anneal the lipid dispersions and to rapidly equilibrate buffer salts throughout the aqueous compartments separating the lipid lamellar stacks (Mayer et al., 1985). The initial heating scans of freshly prepared dispersions of 18:0 LacCer invariably showed a major endothermic peak near 79°C ($\Delta H \cong 14$ kcal/mol), along with a smaller peak at 83–85°C. Subsequent heating scans obtained after incubating 18:0 LacCer dispersions at 5°C for 100 min revealed a dramatic increase in complexity of the melting behavior (Fig. 1), including two new endothermic shoulder peaks at ~80°C and ~81°C. Also, a small exothermic peak was evident near 65–67°C. Heating scans obtained after incubating the same dispersions at 5°C for 12 h or at room temperature for more than 3 days produced no further change in the thermotropic behavior of 18:0 LacCer.

The 16:0 LacCer showed a very sharp endothermic peak near 80°C ($\Delta H \cong 16$ kcal/mol) and a minor endothermic peak at 66–68°C (Fig. 2). Unlike 18:0 LacCer, subsequent heating scans showed essentially the same behavior regardless of whether the sample was cooled and incubated for either 1.7 h or 12 h at 5°C or kept for 3 days at room temperature. Such incubation conditions had previously been shown to significantly affect the thermotropic response of GalCers containing certain homogeneous monounsaturated acyl chains (Kulkarni and Brown, 1998).

To gain insight into the intermolecular packing of 18:0 LacCer and 16:0 LacCer, Langmuir film balance studies were performed at various constant temperatures between 24 and 35°C. Both the surface pressure (π) and the surface compressional modulus (C_s^{-1}) were analyzed as a functional of molecular cross-sectional area (A) for 18:0 LacCer and 16:0 LacCer (Figs. 3 and 4, respectively). At 24°C, 18:0 LacCer and 16:0 LacCer displayed condensed behavior at

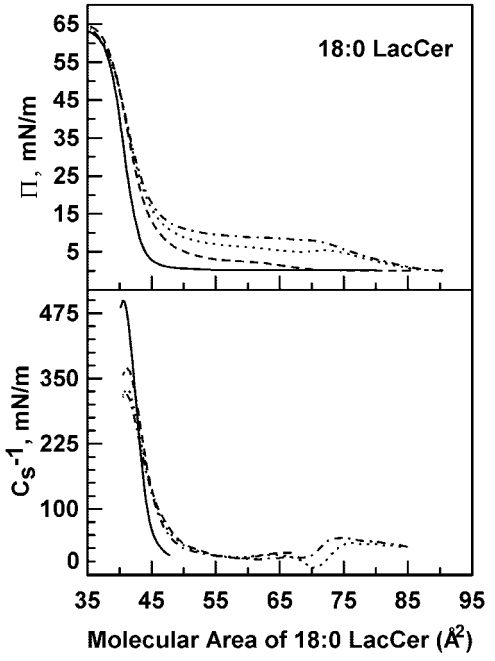

FIGURE 3 18:0 LacCer monolayers. Data were collected using an automated Langmuir-type film balance (see Methods). *Top:* surface pressure versus average cross-sectional molecular area. *Bottom:* surface compressional modulus (C_s^{-1}) versus average molecular area. The isotherm at 24°C is indicated by the solid line; at 30°C, by the dashed line; at 33°C, by the dotted line; and at 35°C, by the dashed-dotted line.

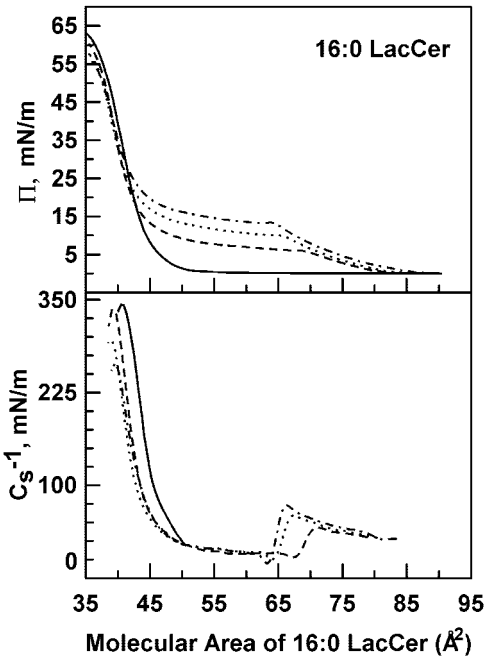

FIGURE 4 16:0 LacCer monolayers. Data were collected using an automated Langmuir-type film balance (see Methods). *Top:* surface pressure versus average cross-sectional molecular area. *Bottom:* surface compressional modulus (C_s^{-1}) versus average molecular area. (Other details are the same as described in Fig. 3 legend.)

all surface pressures between 1 mN/m and collapse. At higher temperatures, two-dimensional phase (2D) transitions of a liquid-expanded (chain-disordered) to condensed (chain-ordered) nature were evident. Figs. 3 and 4 show that, as temperature decreased, the 2D phase transition onset occurred at lower surface pressures (and larger molecular areas). The C_s^{-1} values dropped dramatically at the onsets of the phase transitions of 16:0 LacCer and 18:0 LacCer. As noted previously (Smaby et al., 1996a; Ali et al., 1998; Li et al., 2000), the sharp decline in the C_s^{-1} values upon entering the transition region reflects the difference in the partial molar area within the coexisting liquid-expanded (chain-disordered) and condensed (chain-ordered) phases. Upon completion of the 2D transition, relatively high C_s^{-1} values were observed, consistent with condensed (i.e., gel phase) behavior. At surface pressures mimicking biomembranes (e.g., 30 mN/m), the C_s^{-1} values for 16:0 LacCer and 18:0 LacCer were 328 mN/m and 485 mN/m, respectively (Table 1).

24:0 LacCer and 8:0 LacCer

To determine the effect that marked chain-length asymmetry has on LacCer's thermotropic behavior, DSC experiments were carried out using LacCer that had either very long (24:0) or very short (8:0) *N*-linked acyl chains. It is worth noting that LacCer's 18-carbon sphingoid base provided an effective chain length approximately equivalent to a 14-carbon, saturated *sn*-1 acyl chain in phosphoglycerides (e.g., Li et al., 2001). Figs. 5 and 6 show the thermotropic behavior of 24:0 LacCer and of 8:0 LacCer aqueous dispersions, prepared as described in Materials and Methods. The initial heating scan of 24:0 LacCer was characterized by a single, sharp, endothermic peak with a phase transition temperature at 88°C and total enthalpy (ΔH) of ~14 kcal/mol (Fig. 5). Subsequent heating scans obtained after incubating 24:0 LacCer dispersions at 5°C for 100 min revealed an increase in complexity of the melting behavior. A new low-enthalpy, endothermic transition peak also was evident at 82°C. The main transition peak remained unchanged with respect to temperature, but the enthalpy was reduced. Subsequent heating scans obtained after incubating these same dispersions at 5°C for 12 h or at room temperature (23°C) for 3 days were unchanged.

The behavior of 8:0 LacCer differed markedly from that of 24:0 LacCer. When subjected to the same thermal cycling conditions, 8:0 LacCer dispersions always showed a main phase transition at 45°C ($\Delta H \cong 10$ kcal/mol) and all subsequent heating scans obtained at 10°C/h were identical irrespective of thermal history or incubation conditions. Fig. 6 illustrates the preceding pattern of behavior in heating scans obtained with freshly prepared 8:0 LacCer and after

TABLE 1 Comparison of surface compressibility moduli for LacCer and related sphingolipids at 30 mN/m

Lipid Species	Temp (°C)	Phase State*	Molecular Area (Å^2)	C_s^{-1} (mN/m)	Lipid Species	Temp (°C)	Phase State*	Molecular Area (Å^2)	C_s^{-1} (mN/m)
8:0 LacCer	10	L	60.2	115	24:1 LacCer	15	C	42.3	310
	15	L	58.2	113		20	M	41.1	220
	20	L	56.0	111		24	M	42.7	144
	24	L	61.6	113					
					18:1 LacCer	10	L	49.5	111
16:0 LacCer	24	C	40.8	328		15	L	49.6	113
	30	C	40.5	284		20	L	50.2	116
	33	C	40.6	233		24	L	51.6	116
	35	M	40.9	187					
					16:0 SM	24	M	47.4	196
18:0 LacCer	24	C	40.4	485	18:0 SM	24	M	47.1	279
	30	C	42.0	351	24:0 SM	24	M	46.9	187
	33	C	42.1	302	24:1 SM	24	M	59.6	97
	35	C	42.0	270					
					16:0 GalCer	24	C	40.3	611
24:0 LacCer	24	C	40.6	490	18:0 GalCer	24	C	40.2	648
	30	C	39.7	401	24:0 GalCer	24	C	42.2	495
	33	C	40.5	327	24:1 GalCer	24	C	38.0	342
	35	C	40.9	316	18:1 GalCer	24	L	55.8	159

*Phase state: L denotes liquid-expanded (chain-disordered) state; C denotes condensed (chain-ordered) state; M denotes mixture of liquid-expanded and condensed states. Values for SMs are from Li et al. (2000). Values for GalCers, except for 24:0 GalCer, are from Smaby et al. (1996a).

100 min of incubation at 5°C or after extended incubation (3 days or more) at room temperature.

To determine the intermolecular packing of LacCers with marked chain-length asymmetry, monolayer experiments were carried out on 24:0 LacCer and on 8:0 LacCer. Figs. 7 and 8 show the respective effects of changing cross-sectional molecular area on the surface pressure (π) and C_s^{-1} of 24:0 LacCer and of 8:0 LacCer at different fixed temperatures. At 24°C, 24:0 LacCer showed only condensed behavior, i.e., gel phase. At higher temperatures (e.g., 30–35°C), 2D phase transitions were observed. In response to increasing temperature, the onset surface pressures of the 2D phase transitions of 24:0 LacCer increased while the onset molecular areas decreased. Despite having one very long saturated chain (e.g., 24:0), the 2D phase transitions persisted over a similar temperature range (24–35°C) as observed for much less asymmetric species, i.e., 18:0 LacCer. At temperatures where the isotherms showed 2D phase

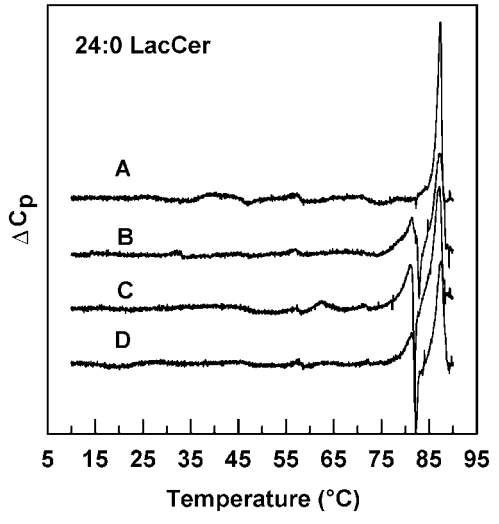

FIGURE 5 DSC of 24:0 LacCer. All traces represent heating scans obtained at a rate of 10°C/h. (Incubation times and temperatures are the same as described in Fig. 1 legend.)

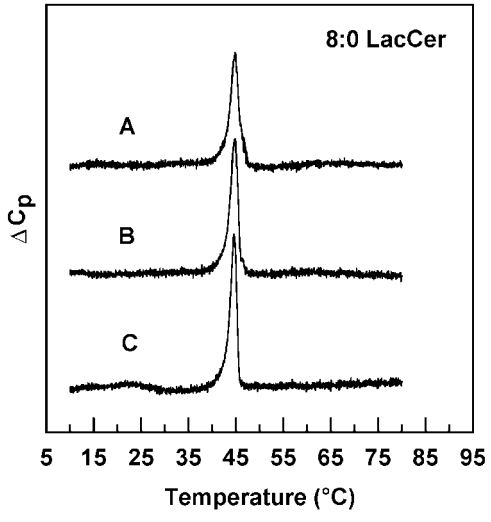

FIGURE 6 DSC of 8:0 LacCer. (*A*) Freshly prepared 16:0 LacCer dispersions incubated 3 h at 5°C before initiating the heating scan; (*B*) 16:0 LacCer dispersions incubated for 100 min at 5°C following an initial heating scan as described in *A*; (*C*) 16:0 LacCer dispersions incubated for 4 days at room temperature (23°C) following the heating scan described in *B*.

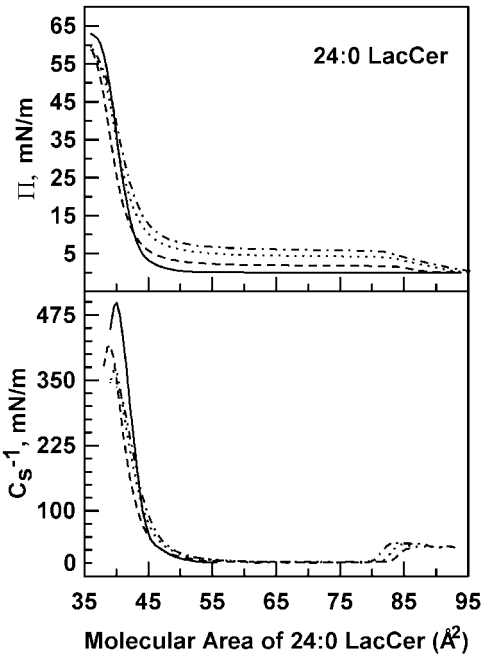

FIGURE 7 24:0 LacCer monolayers. *Top:* surface pressure versus average cross-sectional molecular area. *Bottom:* surface compressional modulus (C_s^{-1}) versus average molecular area. (Other details are the same as described in Fig. 3 legend.)

transitions (e.g., 30–35°C), dramatic drops in the C_s^{-1} values were observed at the onset of the phase transition of 24:0 LacCer. Upon completion of the 2D transition, much higher C_s^{-1} values were evident, consistent with condensed (i.e., gel phase) behavior. At a surface pressure of 30 mN/m and at 24°C, the C_s^{-1} value for 24:0 LacCer was 490 mN/m compared to values of 328 mN/m and 485 mN/m for 16:0 LacCer and 18:0 LacCer, respectively.

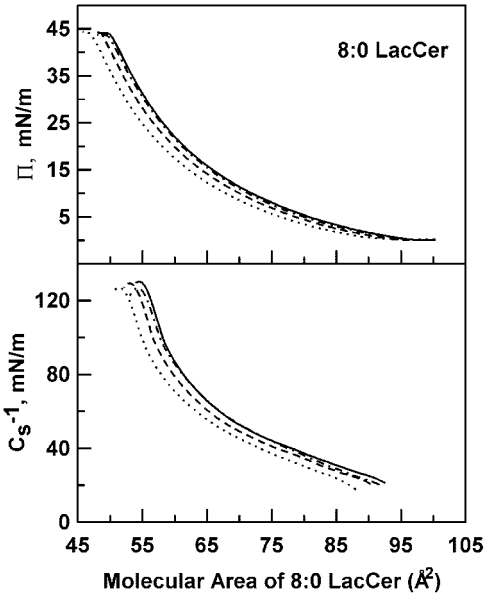

FIGURE 8 8:0 LacCer monolayers. *Top:* surface pressure versus average cross-sectional molecular area. *Bottom:* surface compressional modulus (C_s^{-1}) versus average molecular area. The isotherm at 10°C is indicated by the solid line; at 15°C, by the dashed line; at 20°C, by the dotted line; and at 24°C, by the dashed-dotted line.

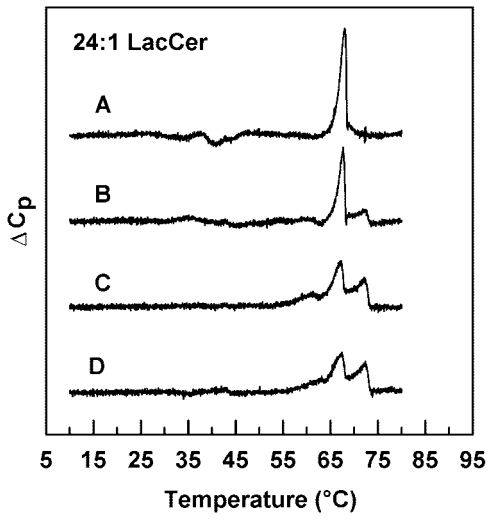

FIGURE 9 DSC of 24:1 LacCer. All traces represent heating scans obtained at a rate of 10°C/h. (Incubation times and temperatures are the same as described in Fig. 1 legend.)

As shown in Fig. 8, liquid-expanded behavior is observed for 8:0 LacCer at all temperatures in the 10–24°C range without any indication of 2D phase transitions. Changing temperature had minimal impact on the C_s^{-1} versus area behavior of 8:0 LacCer. At high surface pressures, such as those that mimic biomembrane conditions (e.g., 30 mN/m), the C_s^{-1} values for fluid-phase 8:0 LacCer were consistently lower (115 mN/m) than those of condensed-phase 16:0 LacCer (260 mN/m).

24:1 LacCer and 18:1 LacCer

To compare the consequences of acyl monounsaturation motifs commonly found in LacCer in nature on LacCer thermotropic behavior, we investigated $24{:}1^{\Delta 15}$ LacCer and $18{:}1^{\Delta 9}$ LacCer by DSC. As shown in Fig. 9, the initial heating scans of freshly prepared 24:1 LacCer dispersions were characterized by a single endothermic peak at 68°C ($\Delta H \cong 9$ kcal/mol). Subsequent heating scans, with samples equilibrated at 5°C for 100 min, showed a major endothermic peak at 68°C and a minor endothermic peak at 72°C. Heating scans obtained after incubation of these same dispersions at 5°C for 12 h also showed two distinct endothermic peaks at 68°C and 72°C. The heating thermogram of 24:1 LacCer remained unchanged even after extended incubation (4 days or more) at room temperature. The behavior of 24:1 LacCer was of particular relevance because the nervonoyl acyl chain (24 carbons with one *cis* double bond

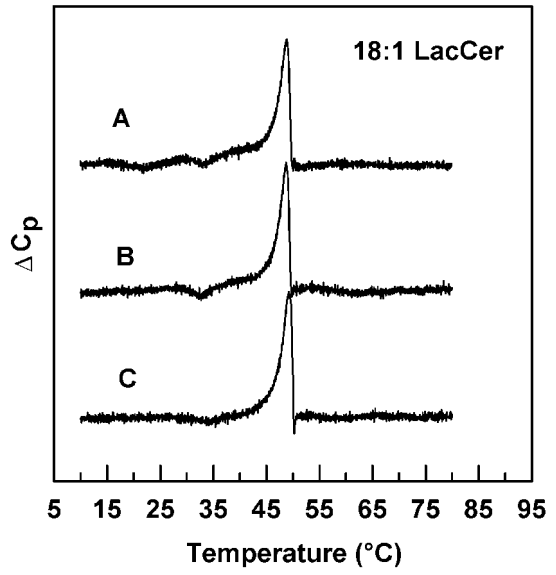

FIGURE 10 DSC of 18:1 LacCer. All traces represent heating scans obtained at a rate of 10°C/h. (Incubation times and temperatures are the same as described in Fig. 6 legend.)

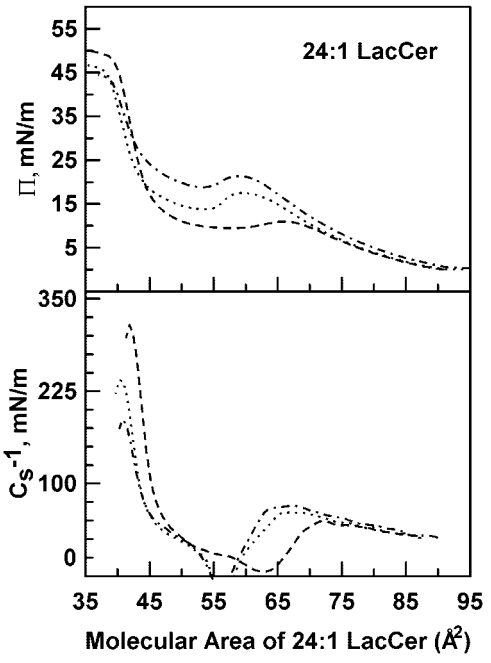

FIGURE 11 24:1 LacCer monolayers. *Top:* surface pressure versus average cross-sectional molecular area. *Bottom:* surface compressional modulus (C_s^{-1}) versus average molecular area. (Other details are the same as described in Fig. 8 legend.)

at carbon 15) is a very common unsaturated chain in naturally occurring LacCer.

Fig. 10 shows the heating scans of 18:1 LacCer aqueous dispersions prepared by the same freeze-thaw procedure used throughout this study. As with 8:0 LacCer, subjecting 18:1 LacCer dispersions to the same thermal history as other LacCer derivatives produced heating thermograms that were very similar. In the case of 18:1 LacCer, the first and subsequent heating scans were identical. A main phase transition was evident at 49°C ($\Delta H \cong 11$ kcal/mol). Incubation of 18:1 LacCer at 5°C for either 100 min or 12 h or at room temperature for 4 days produced no change in the position of the main transition peak or in the transition enthalpy.

To determine the effect of locating a single *cis* double bond two-thirds of the way down a very long acyl chain ($24{:}1^{\Delta 15}$) versus locating a single *cis* double bond in the middle of a long acyl chain (e.g., $18{:}1^{\Delta 9}$), we investigated LacCer intermolecular packing at various fixed temperatures using the surface balance; 24:1 LacCer exhibited 2D phase transitions at 15, 20, and 24°C (Fig. 11). The C_s^{-1} value of 24:1 LacCer at 30 mN/m (15°C) was 310 mN/m, consistent with condensed, chain-ordered phase behavior. With 18:1 LacCer (Fig. 12), liquid-expanded behavior was observed at all temperatures in the 10–24°C range and changing temperature exerted little effect on the C_s^{-1} versus area behavior. The C_s^{-1} values for 18:1 LacCer at 30 mN/m were similar to those of 8:0 LacCer (113–118 mN/m range), consistent with fluid, chain-disordered phase behavior.

DISCUSSION

The present study provides fundamental insights into the physical behavior of LacCer and emphasizes the contributions that the disaccharide headgroup and ceramide structure make to the phase behavior of this glycosphingolipid. Obtaining such insights has become increasingly important due to the emerging roles of LacCer in raft formation and stabilization, as well as in various cell signaling processes (see Introduction). By synthesizing several LacCers with different homogeneous acyl chains and investigating their behavior by the DSC and monolayer approaches, we have clearly identified structural parameters that dominate the phase behavior and lateral packing interactions of several physiologically relevant species of LacCer. Previously, a limited and fragmented picture of LacCer phase behavior existed because earlier studies involved either biologically derived LacCer containing mixed acyl compositions, or were limited to only two chain-pure LacCer derivatives (e.g., Maggio et al., 1985; Maggio, 1994; Saxena et al., 2000).

LacCer headgroup effects

When viewed within the context of studies of other simple sphingolipids and of related glyceroglycolipids, our findings show LacCer's phase behavior to be unexpectedly intriguing. The main endothermic transition temperatures of

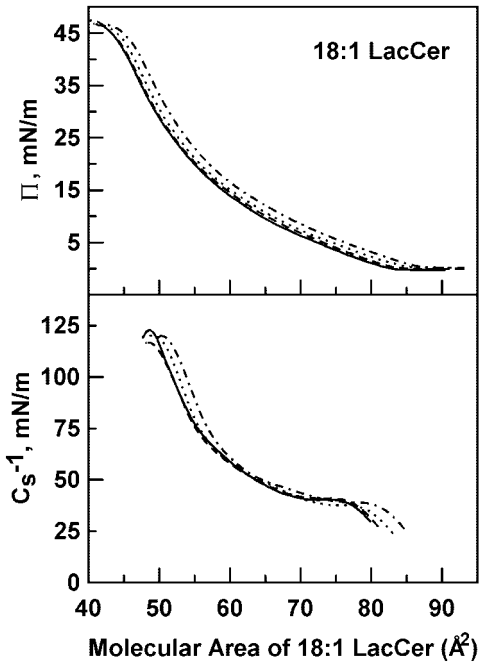

FIGURE 12 18:1 LacCer monolayers. *Top:* surface pressure versus average cross-sectional molecular area. *Bottom:* surface compressional modulus (C_s^{-1}) versus average molecular area. (Other details are the same as described in Fig. 8 legend.)

LacCer containing long saturated acyl chains (e.g., 16:0, 18:0, or 24:0) are relatively high (Table 2) and similar to values previously reported for the corresponding GalCer derivatives (e.g., Koynova and Caffrey, 1995). Thus, the presence of the uncharged disaccharide headgroup in LacCer only marginally affects the main endothermic phase transition temperature despite the lactose headgroup being substantially larger than that of galactose in GalCer. This situation markedly contrasts that of glycosphingolipids with more complex sugar headgroups (Maggio et al., 1985) and that of sphingomyelins (SMs) containing palmitoyl, stearoyl, or lignoceroyl acyl chains where the presence of the zwitterionic phosphorylcholine headgroup lowers the main endothermic phase transition by ~40°C (e.g., Koynova and Caffrey, 1995). The marginal capability of the lactose disaccharide headgroup to disrupt the stable gel phase of LacCer is noteworthy because glycerol-based glycolipids such as digalactosyldiglyceride do not share this feature. Rather, the presence of the disaccharide sugar headgroup in the glycerol-based glycolipids dramatically lowers the phase transition temperature compared to chain-matched diglycerides containing monosaccharide headgroups (Sen et al., 1981, 1983, 1990; Hinz et al., 1991, Mannock et al., 1994). On an absolute basis, the main endothermic transition temperature of 18:0 LacCer is ~30°C higher than that of di-18:0 digalactosyldiglyceride, while 18:0 GalCer's main endothermic transition temperature is only a few degrees higher than that of 18:0 monogalactosyldiglyceride (Sen et al., 1983; Reed and Shipley, 1989; Koynova and Caffrey, 1995). Thus, the especially stable nature of LacCer with long saturated acyl chains appears to originate from a combination of contributions linked to the lactose headgroup and to the ceramide region.

TABLE 2 Phase characteristics of lactosylceramides and sphingomyelins

Lipid	$d\pi/dT$	T_o (°C)	T_m (°C)	
16:0 LacCer	1.08	26.9	66–68	79–81
18:0 LacCer	0.65	28.2	78–80	83–85
24:0 LacCer	0.51	27.9	81–82	87–88
24:1 LacCer	0.96	7.2	67–68	71–72
16:0 SM	1.35	13.0	40.5	
18:0 SM	1.32	18.8	44.7	
24:0 SM	0.72	18.2	47.1	
24:1 SM	0.91	−4.6	26.2	

Values for $d\pi/dT$ and T_o (°C) were calculated from the slopes and x-intercepts, respectively, of the T_o (°C) best-fit lines to the phase transition onset surface pressure versus temperature plots (Kellner et al., 1978). The phase transition onset surface pressures were determined from the C_s^{-1}-A plots. Values for SMs are from Li et al. (2000). The T_m for LacCer includes the temperatures of the two major endotherms observed under various incubation conditions described in the text.

An intriguing but not surprising finding is the complex and metastable thermotropic behavior displayed by certain LacCer species. Such behavior is typical of some, but not all, sphingolipid derivatives (Estep et al., 1980; Boggs et al., 1988; Reed and Shipley, 1989). For example, the main endothermic transition of 18:1 GalCer depends upon sample history and incubation temperature (Reed and Shipley, 1989). If incubated two or more times at temperatures between 45 and 55°C, a time-dependent transformation to a higher melting form ($T_m \cong 55$°C) occurs. However, a lower melting form ($T_m \cong 45$°C) dominates if the 18:1 GalCer is cooled and incubated well below 45°C. Because our initial heating scan of 18:0 LacCer clearly showed a small endothermic peak near 83–85°C, in addition to the major peak near 79°C, we tested whether similar manipulations could be used to convert 18:0 LacCer to the higher melting phase. Fig. 13 shows that such a conversion does occur (*top panel*, scan *A*) when 18:0 LacCer is successively cycled two or more times in the following way: initial heating scan, maintain at 80–85°C for 3–4 h, cool for 2 h at 5°C, and rescan to 90°C. Fig. 13 (scan *B* of *top panel*) shows that simply cooling 18:0 LacCer for 2 h at 5°C (without incubating for 3–4 h at 80–85°C) results in a lower endothermic transition (76–78°C) dominating the scan. Interestingly, when 16:0 LacCer was treated in an identical manner, no shifting of the main endothermic transition (80–81°C) to higher or lower temperatures was observed (Fig. 13, *bottom panel*). However, the small endothermic peak near 66–68°C did diminish after incubating for 3–4 h at 80–85°C (Fig. 13, *bottom panel*, scan *A*). Saxena et al. (2000) have reported that incubating near 70°C for 2 h, cooling to 10°C, and then heat-scanning upward generates the higher melting endo-

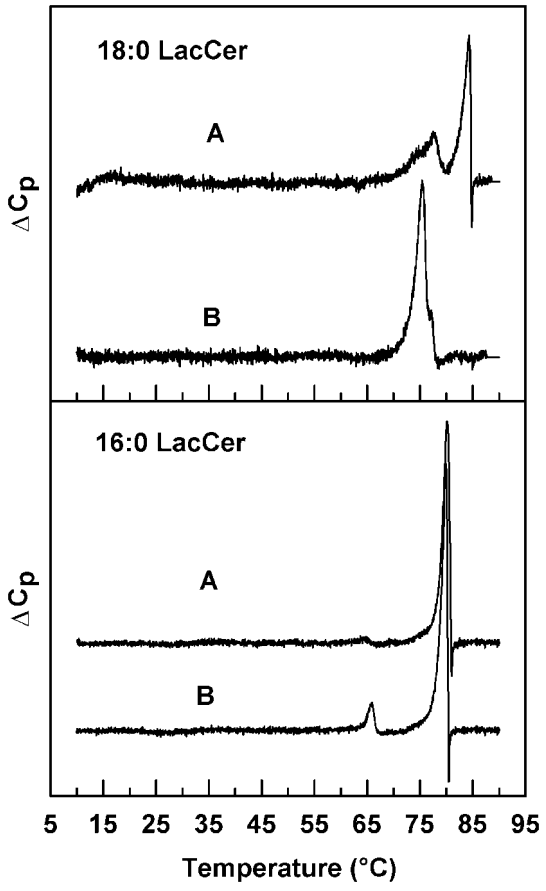

FIGURE 13 DSC metastability analyses of 18:0 LacCer and 16:0 LacCer. *Top:* 18:0 LacCer (1.2 mM); scan *A* was obtained after preparing fresh sample and scanning as in Fig. 1 *A*, and then cyclically incubating at 80–85°C for 3–4 h, cooling to 5°C for 2 h, and rescanning to 90°C at least two or more times. Scan *B* was obtained when the scan *A* sample was then simply cooled to 5°C for 2 h and rescanned to 90°C (without including the 80–85°C incubation step). *Bottom:* 16:0 LacCer (1.2 mM), scans *A* and *B* performed exactly as described for 18:0 LacCer in the top panel.

thermic peak in 16:0 LacCer, whereas heating to 90°C and cooling to 10°C, without incubating near 70°C, produces three overlapping transitions in the 66–72°C range. Diffraction analyses indicate differences in the molecular tilt and hydration among the various bilayer polymorphs of 16:0 LacCer. Clearly, a comprehensive study that includes structural analyses will be required to fully characterize the different bilayer polymorphs formed by the various LacCer species described here.

The monolayer data provide insights not only into the phase behavior, but also into the intermolecular packing of the LacCers. Consistent with the DSC data, the effect of different fixed temperatures on the 2D phase behavior of LacCers with long saturated acyl chains more closely parallels that of corresponding GalCers than that of SMs (Fidelio et al., 1986; Ali et al., 1991, 1993, 1994; Li et al., 2000). The LacCers require relatively high temperatures (>24°C) to undergo 2D phase transitions; whereas lower temperatures are sufficient for SM. Table 2 provides a comparison of the temperature at which the transition onset (T_o) first becomes evident for the LacCers and for the corresponding chain-matched SMs (Li et al., 2000). The T_o values for the LacCers (16:0, 18:0, and 24:0) are ~10°C higher than those of the SMs, an observation consistent with increased van der Waals stabilization in the LacCers. Previously, we showed that SMs containing palmitoyl, stearoyl, or lignoceroyl acyl chains have similar T_o values. This also is the case for LacCer derivatives with corresponding acyl chains. In contrast, in bilayers, the T_m values increase moderately with increasing chain length for the 16:0, 18:0, and 24:0 derivatives. This response may reflect added stabilization that occurs in bilayers, but not in monolayers, via chain interdigitation as LacCer's chain length asymmetry increases.

The surface compressional moduli, which provide a quantitative measure of lipid in-plane packing elasticity, show the condensed phase of LacCer with long saturated acyl chains to be very tightly packed in an in-plane sense at high surface pressures (30 mN/m) that mimic the biomembrane situation, consistent with enhanced van der Waals interactions achieved in the chain-ordered state. At equivalent surface pressure and temperature in the chain-ordered state, the LacCer films are less elastic than SM films, but are somewhat more elastic than GalCer films (Table 1). The relatively high packing density of LacCer is interesting because the ceramide structures are matched and the only difference is one additional sugar in the headgroup compared to GalCer. Because differing hydrated bulk volume and average orientation of the polar headgroups can alter the average molecular area and molecular packing elasticity (e.g., Maggio, 1994; Ali et al., 1993), increasing the headgroup size from one sugar to two sugars would be expected to increase the elasticity among LacCer molecules by limiting the intermolecular approach compared with the smaller, less hydrated GalCer. This scenario would be especially true if the lactose headgroup orients roughly orthogonal to its hydrocarbon chains and parallel to the air-water interface. However, the monolayer and DSC data only marginally support the preceding view for LacCer, particularly at high surface pressures that mimic biomembrane conditions. The data are consistent with the lactose headgroup extending more perpendicular than parallel to the bilayer plane, with the relatively flat pyranose rings minimizing packing disruption by lying within the same plane in the stable gel phase. Such headgroup arrangement may be facilitated by intermolecular lactose-lactose interactions (Yu et al., 1997) that can be promoted by the sphingosine functional groups of the interfacial region (e.g., hydroxyl and amide linkage) and by the long and saturated acyl chains. Although SMs with saturated chains also share the same features of the ceramide region, the high hydration capacity of the phosphorylcholine residue deriving from the ionic phosphate and amine groups, coupled with the more

parallel orientation to interfacial region, increase steric bulkiness with respect to neighboring lipids. This effectively limits the intermolecular interactions of SMs and may restrict the intermolecular hydrogen-bonding capability provided by the amide linkage and hydroxyl group of ceramide. The result is a substantially destabilized gel phase and significantly lowered transition temperatures for saturated SMs compared to either saturated GalCers or saturated LacCers. Our conclusions are supported by monolayer data describing SM and GalCer behavior (Johnston and Chapman, 1988; Lund-Katz et al., 1988; Ali et al., 1991, 1993, 1994; Smaby et al., 1996a; Ramstedt and Slotte, 1999; Li et al., 2000).

LacCer acyl chain structural effects

In light of the rather modest response of LacCer's major endothermic transition temperature(s) to changes in saturated acyl chain length (e.g., 16:0, 18:0, or 24:0 LacCer), the results obtained with LacCer containing nervonate ($24{:}1^{\Delta 15}$) and oleate ($18{:}1^{\Delta 9}$) are particularly interesting. With both of these physiologically relevant monounsaturated LacCer derivatives, substantially lower main endothermic transition temperatures are observed relative to their saturated counterparts, although a greater reduction in the transition temperature occurs in 18:1 LacCer (T_m = 49°C) than in 24:1 LacCer (T_m = 68°C). The monolayer isotherms agree with the DSC data in that 18:1 LacCer shows only liquid-expanded behavior at all temperatures in the 10–24°C range, while 24:1 LacCer shows 2D transitions at 15, 20, or 24°C. The metastable nature of the 24:1 LacCer phase transition is clearly evident in the 20°C and 24°C isotherms and in the DSC thermograms (Fig. 9). Similar metastable behavior has been reported for 24:1 GalCer monolayers and bilayers (Ali et al., 1993; Kulkarni et al., 1995; Smaby et al., 1996a; Kulkarni and Brown, 1998). In contrast, neither the monolayer isotherms nor the DSC thermograms for 18:1 LacCer show evidence of metastability, a result consistent with earlier observations of 18:1 GalCer behavior (Ali et al., 1991, 1993; Smaby et al., 1996a; Kulkarni and Brown, 1998).

The presence of a *cis* double bond in an acyl chain is known to introduce a "crankshaft"-type *trans-gauche* kink into the hydrocarbon chain (Lagaly et al., 1977). Such a kink can be expected to disrupt chain-chain packing, increase the average cross-sectional area of LacCer, and increase the in-plane elasticity. Under such circumstances, LacCer hydration may be affected and intermolecular hydrogen-bonding interactions diminished. Our monolayer data are consistent with the preceding scenario.

IMPLICATIONS

The tendency of certain GSLs to associate into membrane microdomains when mixed with other lipids in model membranes was recognized many years ago (Thompson and Tillack, 1985). Recent extensions of these ideas have led to the membrane "raft" concept, in which microdomains enriched in sphingolipids and cholesterol function as organizing platforms for proteins with certain types of lipid anchors (Simons and Ikonen, 1997; Brown, 1998; Brown and London, 2000). The liquid-ordered environment within rafts is thought to be a key feature that controls the extent to which lipid-anchored proteins localize to rafts and limits solubilization by Triton X-100 (Brown and London, 2000; Li et al., 2001). Given the observation that the acyl chain composition of naturally occurring LacCers often is highly enriched in stearoyl chains, the physical features that we describe for LacCer are consistent with localization to the detergent-insoluble membrane fraction isolated from cells. Moreover, by having a sugar headgroup that extends beyond that of many other lipid molecules (e.g., phosphoglycerides, cholesterol, sphingomyelins), it is tempting to speculate that LacCer may be among a select group of lipids that can trigger raft-related signal transduction processes by attracting soluble proteins that possess carbohydrate binding sites.

We are grateful to an anonymous reviewer for suggesting experimental ways to address metastability issues that are important for clarifying data presented in Table 2.

This investigation was supported by U.S. Public Health Service (USPHS) Grant GM45928 (to R.E.B.) and the Hormel Foundation. The automated Langmuir film balance used in this study received major support from USPHS Grant HL49180 (to H.L.B.).

REFERENCES

Albon, N., and J. F. Baret. 1983. Comparisons and correlations between the properties of lipid molecules in crystals, bilayer dispersions in water, and monolayers on a water surface. *J. Colloid Interface Sci.* 92:545–560.

Ali, S., H. L. Brockman, and R. E. Brown. 1991. Structural determinants of miscibility in surface films of galactosylceramide and phosphatidylcholine: effect of unsaturation in the galactosylceramide acyl chain. *Biochemistry.* 30:11198–11205.

Ali, S., J. M. Smaby, H. L. Brockman, and R. E. Brown. 1994. Cholesterol's interfacial interactions with galactosylceramides. *Biochemistry.* 33:2900–2906.

Ali, S., J. M. Smaby, and R. E. Brown. 1993. Acyl structure regulates galactosylceramide's interfacial interactions. *Biochemistry.* 32: 11696–11703.

Ali, S., J. M. Smaby, M. M. Momsen, H. L. Brockman, and R. E. Brown. 1998. Acyl chain-length asymmetry alters the interfacial elastic interactions of phosphatidylcholines. *Biophys. J.* 74:338–348.

Angstrom, J., S. Teneberg, M. A. Milh, T. Larsson, I. Leonardsson, B. M. Olsson, M. O. Halvarsson, D. Danielsson, I. Naslund, A. Ljungh, T. Wadstrom, and K. A. Karlsson. 1998. The lactosylceramide binding specificity of *Helicobacter pylori*. *Glycobiology.* 8:297–309.

Behroozi, F. 1996. Theory of elasticity in two dimensions and its application to Langmuir-Blodgett films. *Langmuir.* 12:2289–2291.

Boggs, J. M., K. M. Koshy, and G. Rangaraj. 1988. Influence of structural modifications on the phase behavior of semi-synthetic cerebroside sulfate. *Biochim. Biophys. Acta.* 938:361–372.

Brown, R. E. 1998. Sphingolipid organization in biomembranes: what physical studies of model membranes reveal. *J. Cell Sci.* 111:1–9.

Brown, D. A., and E. London. 1998. Functions of lipid rafts in biological membranes. *Annu. Rev. Cell and Dev. Biol.* 14:111–136.

Brown, D. A., and E. London. 2000. Structure and function of sphingolipid- and cholesterol-rich membrane rafts. *J. Biol. Chem.* 275: 17221–17224.

Brown, D. A., and J. K. Rose. 1992. Sorting of GPI-anchored proteins to glycolipid-enriched membrane subdomains during transport to the apical cell surface. *Cell.* 68:533–544.

Chatterjee, S. 1998. Sphingolipids in atherosclerosis and vascular biology. *Arterioscler. Thromb. Vasc. Biol.* 18:1523–1533.

Chen, C. S., M. C. Patterson, C. L. Wheatley, J. F. O'Brien, and R. E. Pagano. 1999. Broad screening test for sphingolipid-storage diseases. *Lancet.* 354:901–905.

Davies, J. T., and E. K. Rideal. 1963. Interfacial Phenomena, 2nd Ed. Academic Press, New York. 265.

Estep, T. N., W. I. Calhoun, Y. Barenholz, R. L. Biltonen, G. G. Shipley, and T. E. Thompson. 1980. Evidence for metastability in stearoylsphingomyelin bilayers. *Biochemistry.* 19:20–24.

Evans, E., and D. Needham. 1987. Physical properties of surfactant bilayer membranes: thermal transitions, elasticity, rigidity, cohesion, and colloidal interactions. *J. Phys. Chem.* 91:4219–4228.

Fidelio, G. D., B. Maggio, and F. A. Cumar. 1986. Molecular parameters and physical state of neutral glycosphingolipids and gangliosides in monolayers at different temperatures. *Biochim. Biophys. Acta.* 854: 231–239.

Hakomori, S., and Y. Igarashi. 1995. Functional role of glycosphingolipids in cell recognition and signaling. *J. Biochem.* 118:1091–1103.

Hinz, H.-J., H. Kutternreich, R. Meyer, M. Renner, R. Frund, R. Koynova, A. I. Boyanov, and B. G. Tenchov. 1991. Stereochemistry and size of sugar headgroups determine structure and phase behavior of glycolipid membranes: densitometric, calorimetric and x-ray studies. *Biochemistry.* 30:5125–5138.

Huwiler, A., T. Kolter, J. Pfeilschifter, and K. Sandhoff. 2000. Physiology and pathophysiology of sphingolipid metabolism and signaling. *Biochim. Biophys. Acta.* 1485:63–99.

Iwamoto, T., S. Fukumoto, K. Kanaoka, E. Sakai, M. Shibata, E. Fukumoto, J. Inokuchi, K. Takamiya, K. Furukawa, K. Furukawa, Y. Kato, and A. Mizuno. 2001. Lactosylceramide is essential for the osteoclastogenesis mediated by macrophage-colony-stimulating factor and receptor activator of nuclear factor-κB ligand. *J. Biol. Chem.* 49: 46031–46038.

Johnston, D. S., and D. Chapman. 1988. A calorimetric study of the thermotropic behaviour of mixtures of brain cerebrosides with other brain lipids. *Biochim. Biophys. Acta.* 939:603–614.

Kaganer, V. M., H. Möhwald, and P. Dutta. 1999. Structure and phase transitions in Langmuir monolayers. *Rev. Mod. Physics.* 71:779–819.

Koynova, R., and M. Caffrey. 1995. Phases and phase transitions of the sphingolipids. *Biochim. Biophys. Acta.* 1255:213–236.

Kulkarni, V. S., W. H. Anderson, and R. E. Brown. 1995. Bilayer nanotubes and helical ribbons formed by hydrated galactosylceramides: acyl chain and headgroup effects. *Biophys. J.* 69:1976–1986.

Kulkarni, V. S., and R. E. Brown. 1998. Thermotropic behavior of galactosylceramides with cis-monoenoic fatty acyl chains. *Biochim. Biophys. Acta.* 1372:347–358.

Lagaly, G., A. Weiss, and E. Stuke. 1977. Effect of double-bonds on bimolecular films in membrane models. *Biochim. Biophys. Acta.* 470: 331–341.

Li, X-M., M. M. Momsen, J. M. Smaby, H. L. Brockman, and R. E. Brown. 2001. Cholesterol decreases the interfacial elasticity and detergent solubility of sphingomyelins. *Biochemistry.* 40:5954–5963.

Li, X-M., M. Ramakrishnan, H. L. Brockman, R. E. Brown, and M. J. Swamy. 2002. *N*-myristoylated phosphatidylethanolamine: interfacial behavior and interaction with cholesterol. *Langmuir.* 18:231–238.

Li, X-M., J. M. Smaby, M. M. Momsen., H. L. Brockman, and R. E. Brown. 2000. Sphingomyelin interfacial behavior: the impact of changing acyl chain composition. *Biophys. J.* 78:1921–1931.

Lund-Katz, S., H. M. Laboda, L. R. McLean, and M. C. Phillips. 1988. Influence of molecular packing and phospholipid type on rates of cholesterol exchange. *Biochemistry.* 27:3416–3423.

Maggio, B. 1994. The surface behavior of glycosphingolipids in biomembranes: a new frontier of molecular ecology. *Prog. Biophys. Mol. Biol.* 62:55–117.

Maggio, B., T. Ariga, J. M. Sturtevant, and R. K. Yu. 1985. Thermotropic behavior of glycosphingolipids in aqueous dispersions. *Biochemistry.* 24:1084–1092.

Maggio, B., F. A. Cumar, and R. Caputto. 1978. Surface behavior of gangliosides and related glycosphingolipids. *Biochem. J.* 171:559–565.

Maggio, B., F. A. Cumar, and R. Caputto. 1980. Configuration and interactions of the polar head group in gangliosides. *Biochem. J.* 189: 435–440.

Maggio, B., F. A. Cumar, and R. Caputto. 1981. Molecular behavior of glycosphingolipids in interfaces: possible participation in some properties of nerve membranes. *Biochim. Biophys. Acta.* 650:69–87.

Mannock, D. A., R. N. McElhaney, P. E. Harper, and S. M. Gruner. 1994. Differential scanning calorimetry and x-ray diffraction studies of the thermotropic phase behavior of the diastereomeric di-tetradecyl-β-D-galactosyl glycerols and their mixtures. *Biophys. J.* 66:734–740.

Mayer, L. D., M. J. Hope, P. R. Cullis, and A. S. Janoff. 1985. Solute distributions and trapping efficiencies observed in freeze-thawed multilamellar vesicles. *Biochim. Biophys. Acta.* 817:193–196.

Momsen, W. E., J. M. Smaby, and H. L. Brockman. 1990. The suitability of nichrome for measurement of gas-liquid interfacial tension by the Wilhelmy method. *J. Colloid Interface Sci.* 135:547–552.

Needham, D. 1995. Permeability and Stability of Lipid Bilayers. E. A. Disalvo and S. A. Simon, editors. CRC Press, Boca Raton, FL. 49–76.

Needham, D., and R. S. Nunn. 1990. Elastic deformation and failure of lipid bilayer membranes containing cholesterol. *Biophys. J.* 58: 997–1009.

Parkin, E. T., A. J. Turner, and N. M. Hooper. 2001. Differential effects of glycosphingolipids on the detergent-insolubility of the glycosylphosphatidylinositol-anchored membrane dipeptidase. *Biochem. J.* 358: 209–216.

Peters, R., and K. Beck. 1983. Translational diffusion in phospholipid monolayers measured by fluorescence microphotolysis. *Proc. Natl. Acad. Sci. U.S.A.* 80:7183–7187.

Phillips, M. C., and D. Chapman. 1968. Monolayer characteristics of saturated 1,2-diacyl phosphatidylcholines (lecithins) and phosphatidylethanolamines at the air-water interface. *Biochim. Biophys. Acta.* 163:301–313.

Pincet, F., T. L. Bouar, Y. Zhang, J. Esnault, J. M. Mallet, E. Perez, and P. Sinay. 2001. Ultraweak sugar-sugar interaction for transient cell adhesion. *Biophys. J.* 80:1354–1358.

Ramstedt, B., and J. P. Slotte. 1999. Interaction of cholesterol with sphingomyelins and acyl-chain-matched phosphatidylcholines: a comparative study of the effect of the chain length. *Biophys. J.* 76:908–915.

Reed, R. A., and G. G. Shipley. 1989. Effect of chain unsaturation on the structure and thermotropic properties of galactocerebrosides. *Biophys. J.* 55:281–292.

Saxena, K., P. Zimmermann, R. R. Schmidt, and G. G. Shipley. 2000. Bilayer properties of totally synthetic C16:0-lactosylceramide. *Biophys. J.* 78:306–312.

Sen, A., S.-W. Hui, D. A. Mannock, R. N. A. H. Lewis, and R. N. McElhaney. 1990. Physical properties of glycosyldiacylglycerols. 2. X-ray diffraction studies of a homologous series of 1,2-Di-*O*-acyl-3-*O*-(α-D-glucopyranosyl)-*sn*-glycerols. *Biochemistry.* 29:7799–7804.

Sen, A., D. A. Mannock, D. J. Collins, and P. J. Quinn. 1983. Thermotropic phase properties and structure of 1,2-distearoylgalactosylglycerols in aqueous systems. *Proc. R. Soc. Lond. A.* 218:349–364.

Sen, A., W. P. Williams, and P. J. Quinn. 1981. The structure and thermotropic properties of pure 1,2-diacylgalactosylglycerols in aqueous systems. *Biochim. Biophys. Acta.* 663:380–389.

Simons, K., and E. Ikonen. 1997. Functional rafts in cell membranes. *Nature.* 387:569–572.

Simons, K., and D. Toomre. 2000. Lipid rafts and signal transduction. *Nat. Rev. Mol. Cell. Biol.* 1:31–39.

Smaby, J. M., and H. L. Brockman. 1991. A simple method for estimating surfactant impurities in solvents and subphases used for monolayer studies. *Chem. Phys. Lipids.* 58:249–252.

Smaby, J. M., V. S. Kulkarni, M. Momsen, and R. E. Brown. 1996a. The interfacial elastic packing interactions of galactosylceramides, sphingomyelins, and phosphatidylcholines. *Biophys. J.* 70:868–877.

Smaby, J. M., M. Momsen, H. L. Brockman, and R. E. Brown. 1997. Phosphatidylcholine acyl unsaturation modulates the decrease in interfacial elasticity induced by cholesterol. *Biophys. J.* 73:1492–1505.

Smaby, J. M., M. Momsen, V. S. Kulkarni, and R. E. Brown. 1996b. Cholesterol-induced interfacial area condensations of galactosylceramides and sphingomyelins with identical acyl chains. *Biochemistry.* 35: 5696–5704.

Thompson, T. E., and T. W. Tillack. 1985. Organization of glycosphingolipids in bilayers and plasma membranes of mammalian cells. *Annu. Rev. Biophys. Chem.* 14:361–381.

van Meer, G., and J. C. M. Holthuis. 2000. Sphingolipid transport in eukaryotic cells. *Biochim. Biophys. Acta.* 1486:145–170.

Weis, W., and K. Drickamer. 1996. Structural basis of lectin-carbohydrate recognition. *Annu. Rev. Biochem.* 65:441–473.

Yu, Z., T. L. Calvert, and D. Leckband. 1997. Molecular forces between membranes displaying neutral glycosphingolipids: evidence for carbohydrate attraction. *Biochemistry.* 37:1540–1550.